Adapted Semi-Regular 3-D Mesh Coding Based on a Wavelet Segmentation

Céline Roudet[a], Florent Dupont[a] and Atilla Baskurt[b]

[a] LIRIS, UMR 5205 CNRS, Université de Lyon, Université Lyon 1, Villeurbanne, F-69622, France.

[b] LIRIS, UMR 5205 CNRS, Université de Lyon, INSA de Lyon, Villeurbanne, F-69621, France.

ABSTRACT

We present a local wavelet decomposition framework based on a segmentation of semi-regular meshes and mostly dedicated to mesh compression purposes. The shape partition has been created to adapt the compression in the regions where the wavelet coefficients have a non negligible magnitude or polar angle (the angle with the normal vector), reflecting the high frequencies of the model. This partitioning have been produced by first applying a classification algorithm (K-Means) on a 3D mesh. Given a segmentation constructed from the latter classification, it is possible to adapt a special treatment on each region, according to its frequency magnitude, in order to produce the smallest wavelet coefficients. The wavelets can also be quantized and encoded independently in order to minimize the global distortion at a given bitrate and provide a very efficient and flexible compression scheme. Finally, the proposed local multiresolution analysis allow the user to reconstruct adaptively the produced patches that generally correspond to relevant parts of the mesh. Several other kind of applications can benefit from this adaptive decomposition, like error resilient compression or watermarking. We present some examples for which the redundancy produced by the partitioning can be compensated by a well adapted prediction scheme on each region.

Keywords: Geometric wavelets, mesh partitioning, multi-resolution analysis, lifting scheme, 3-D mesh compression.

1. INTRODUCTION

With the emerging development of the Internet and the telecommunication networks, the 3D models are more and more widespread. Indeed these kinds of objects are not only used in entertainment (video games or animation films), but also for industrial purposes like medical imaging, car industry (CAD framework), simulation or virtual environment contexts.

The complexity of the 3D models used in computer graphics has recently increased due to the last progress of the sampling techniques. These objects are consequently represented numerically with more and more precision and details for realism purposes. The modelling of such objects or 3D scenes is commonly done thanks to geometric primitives embedded in the 3D Euclidean space. Triangle mesh is actually the most common representation for these objects because it's a well adapted model for many applications and for the rendering process. This representation include geometry and topology information which could be expensive for computation, storage, transmission and rendering tasks, even if the material involved is more and more competitive.

Consequently multiresolution (MR) techniques have emerged, in order to represent data with multiple Levels of Detail (LOD). They are of particular interest for progressive transmission and visualisation purposes, where a coarse approximation can subsequently be further improved depending on the user resources (network, visualisation terminal) and waitings. This scalable representation is commonly produced by a wavelet transform which is also suitable for denoising, filtering or surface editing purposes.

Two different approaches are considered to achieve this task, considering directly the irregular structure or using a remeshing part to produce a semi-regular representation. In this paper, we consider the semi-regular surface representation for the usual models, which generally contains the fewest connectivity and parametric information to encode. As the target applications do not impose a lossless compression scheme, this modelling

is very interesting to benefit from more efficient data structures and processing algorithms which are closer to the ones used for data sampled on regular grids.

The actual state of the art mesh compression methods, presented in Section 2, generally compress the mesh with a global scheme, except for large polygonal meshes composed of millions or billions of vertices where a partitioning and gluing algorithms are commonly used. We propose a new shape decomposition framework that aims at differentiating the analysis for each partition, consequently the work done in mesh partitioning is also presented in Section 2.

We have used a segmentation based on the wavelet coefficient magnitude or polar angle and produced by a global decomposition. Our goal is to construct homogeneous regions according to these criteria that every remeshing or compressing algorithm tend to minimize. But even if the best methods provide non uniform distributions, some non negligible values still remain because they are generally associated to the high frequency parts of the model. Consequently, we propose to adapt the mesh analysis in the created regions where a different kind of treatment can be considered. We present the framework developped in this context in Section 3 with some of our experimental results. They emphasize in the additive information needed for the patch independent coding which can be compensated by an adapted treatment on each type of region.

The possible applications based on this framework are presented in Section 4 with their corresponding results, like compression or watermarking which can benefit from this partitioning in order to apply different marks or subdivision schemes according to the visual aspect of the surface. Moreover, little attention has been paid to the combination of mesh compression and patch decomposition for ROI decoding, whereas it is possible with JPEG 2000 for images. However a view-dependent streaming of large meshes can accelerate their treatments and rendering, where objects or scene parts could be more refined than others. Another interesting point to be noticed is that the partition coding includes additive information that improves the robustness of the data susceptible to encounter transmission errors in the channels, so another possible application can be error-resilient 3D mesh coding.

Finally discussions and ideas for future work are presented in the last Section.

2. RELATED WORK

The proposed algorithm first partitions semi-regular meshes (produced by a remeshing algorithm) according to their associated wavelet coefficients obtained from a global multiresolution analysis. Each coefficient associated to a given resolution level of the hierarchy is important and reveals the high frequencies lost during the coarsification. The goal of this segmentation is to separate regions for which the associated coefficient magnitude or polar angle (the angle between each coefficient and its corresponding surface normal vector) do not have the same magnitude order in order to adapt a different treatment, aiming at reducing the wavelet coefficients to code.

Before detailing our algorithm, we present in this section the existing work done in mesh partitioning and MR analysis.

2.1. State of the art in mesh partitioning

In the past twenty years, much work has been done in shape decomposition because of its utility in many computer graphic applications. These methods are usually designed to solve a specific application problem using different types of techniques which are difficult to compare. Mesh decomposition is used for applications such as collision detection, skeletonization, metamorphosis, animation or modelling by parts, where the object is generally decomposed in regions corresponding to relevant aspects of the surface of the shape (sub-meshes), which are far from our expectations, but described in the comparative study of Attene *et al.*[1]

Another type of applications use segmentation to simplify treatments like texture mapping, parameterization, mesh editing, modeling, deformation or compression on complex meshes with a high genus, for example. These latter treatments are generally faster and less complicated on surface patches homeomorphic to a disc. In this context, most of the existing segmentation algorithms are based on the surface curvature or planarity information to distinguish the relevant parts or to obtain regions gathering common characteristics.

The former methods that have partitioned the object into surface patches having common characteristics have intended to approximate the object by planar faces so as to minimize the approximation error between this element set and the original surface.[2,3] These approximation techniques are particularly useful for mesh simplification and radiosity. Other approaches[4,5] have used the discrete curvature computed in each vertex with a watershed algorithm adapted from those employed in image segmentation. Mangan *et al.*[4] have generalized this algorithm for arbitrary 3D meshes and have used the Gaussian curvature computed in each vertex as watershed altitude. Another measure of curvature was defined by Sun *et al.*[5] based on a principal component analysis of the surface normal vectors in a geodesic window. More recently, Razdan *et al.*[6] have proposed a hybrid approach, which combines the watershed algorithm with a sharp edge extraction. But theses methods tend to extract only regions surrounded by high curvatures and do not handle correctly the boundaries between the patches, which are either fuzzy or jagged. The method developped by Lavoué *et al.*[7] overcomes these drawbacks using a K-Mean[8] classification algorithm instead of the watershed, in order to more precisely detect curvature transitions, particularly on CAD objects.

We propose to adapt the algorithm of Lavoué *et al.*,[7] formerly conceived for the compression of CAD objects, which contain sharp edges and corners that generally separate smooth regions. Our extension uses the same concept based on the production of homogeneous regions, but regarding surface smoothness. This adaptation is able to compress more natural and complex objects this latter algorithm cannot consider. Most state of the art methods used to compress the 3D models have employed the geometric wavelets in a MR framework. Thus we intend to extend this treatment to the partitions obtained by our segmentation contribution. We first present the existing methods using geometric wavelets for semi-regular mesh compression.

2.2. State of the art in multiresolution analysis of semi-regular meshes

MR analysis for triangles meshes with arbitrary topology has been introduced by Lounsbery[9] who has shown that a subdivision scheme can serve as a scaling function basis in order to extend the wavelet theory for irregular sampled signals like meshes. In this context, the canonical quadrisection produced by the subdivision schemes imposes to apply the analysis on semi-regular meshes, considered as functions via the parameterizations intrinsiquely defined by the remeshing part. The compressing algorithm performances are then highly dependent on the quality (smoothness, distortion) of the parameterization used.

The main semi-regular remeshing algorithms rely on the same philosophy, which aim at removing almost all of the connectivity information from the mesh, and also reduce the parametric information, so as to be able to represent the details only with their geometric part. For that purpose, a mesh simplification is used to produce the base complex on which the input model will be parameterized. Then, the resampling step can vary in its construction but is always based on a subdivision connectivity construction. Two different currents are used to produce the base complex having the same topology as the original surface. The main differences can be noticed during the coarse mesh construction, which can be obtained directly from the initial object or by progressive decimations.

2.2.1. Mesh simplification by chartification

For the first current, the parameterization is in general based on the chartification produced to simplify the mesh, aiming at minimizing the distortion when mapping a curved surface to the plane, with an energy function. The first remeshing method[10] proposed in this context has used a partition of the original mesh into Voronoï tiles, computed by taking into account the geodesic distance. The coarse model has been obtained with the dual construction : the Delaunay triangulation. It has been then refined by subdivision steps and additional displacements to obtain a semi-regular approximation of the original form. The missing details have been obtained at each resolution level thanks to a local parameterization, based on harmonic maps. In the same way, Gioia[11] has also proposed a parameterization based on harmonic maps. The method produces a semi-regular mesh from a coarse one obtained by a partitioning process. The principal difference between these two methods is that the latter take more into account the geometric and visual properties of the initial surface during the construction of the coarsest approximation. Gioia experimentally obtained on average twice less wavelet coefficients than with the previous method, for natural and CAD objects, considering the fact that geometric shapes are not just functions. The recent method proposed by Guskov[12] has also followed this philosophy but will be discussed later to be compared with another up-to-date algorithm.

2.2.2. Mesh simplification by progressive decimation

The other class of methods use progressive decimation generally based on constructing a mesh hierarchy thanks to the vertex removal or edge collapse operation. A specific error metric is also used at each decimation step.

The MAPS algorithm[13] was the first to use mesh simplification in order to build the base domain. Vertex removal has been used to progressively build a parameterization of the original object in a hierarchy of meshes. At each step, the vertices chosen to be removed are those that withdraw the fewest geometrical and topological information. Then the conformal mapping consists in expressing the decimated vertices as barycentric coordinates. The Loop subdivision[14] is finally used to produce the semi-regular mesh from the coarsest one. At the end of the simplification process, each vertex in the input mesh is associated to some base complex triangle with appropriate barycentric coordinates.

As the construction of the base complex is not based on a chartification, some people have noticed that a global parameterization could be constructed. This latter remark was exploited by Guskov *et al.* in another famous algorithm[15] that has used a recursive piercing procedure and unlifted Butterfly wavelets to concentrate the high-frequency information along the surface normal. The resulting meshes are ideally suited for progressive compression purposes, because almost all of the geometric details are expressed with a single scalar. This algorithm currently produces one of the best remeshes for compression purposes but only for closed surfaces.

This has recently been adapted[16] for the progressive compression of 3D dynamic mesh sequences. The authors have used some different decimation process and parameterization of the first frame mesh structure into the base complex. Thanks to this remeshing algorithm, they can better compress mesh sequences with important structural changes, by mapping the same connectivity structure to all the frames.

Because most of the previously described algorithms have suffered from smoothness artefacts at patch boundaries, a new class of algorithms have appeared. They tend to construct a globally smooth parameterization not only within each coarser triangle, but also across patch boundaries and corners. The smoothness of the parameterization is directly related to how well the mesh can be compressed, together with providing good approximations and non degenerated mesh elements.

2.2.3. Methods using a globally smooth parameterization

The first method designed in this context[17] has used the same simplification algorithm as MAPS for building the base domain but with a different decimation selection, based on an energy minimization to better control the induced smoothness, shape quality and metric distortion. Inter-fragment transition functions between patches have been used to ensure global smoothness and relaxation over all overlapping charts. Starting from the initial mapping produced by MAPS, the relaxation process builds the final smooth paramaterization to optimize inter-chart continuity. The compression of the produced semi-regular meshes have given comparable and in some cases superior rate/distortion (r/d) performance than those obtained from the Normal Mesh algorithm.

These transition functions have also been considered by Ray *et al.*[18] to construct a quasi conformal parameterization which does not require any prior partition into charts nor cutting. It avoids finding the optimum partition of the mesh surface into charts, which is an open problem. The produced quadrilateral chart layout has the advantage that it follows the principal curvatures of the object.

More recently, Guskov[12] has proposed to split the original input mesh into Voronoï tiles, in order to obtain the simple base domain and the initial mapping. The minimization of a global parametric energy functional is then used to improve the parameterization. Contrary to the preceding method, they construct an open atlas that covers the base mesh and forms a manifold structure for the parameterization construction and the resampling step. It provides comparable results than the previous method in term of r/d performance, after the application of the compression framework of Khodakovsky *et al.*[19] But the main advantage is that the output mesh is constructed automatically without user intervention. Finally, this algorithm provides an anisotropic remesher extension that allows to control the anisotropy of the output meshes.

Once the semi-regular mesh has been constructed with the fewest connectivity and parametric information, efficient data structures and processing algorithms can be used to get closer to the methods used for data sampled on regular grids.
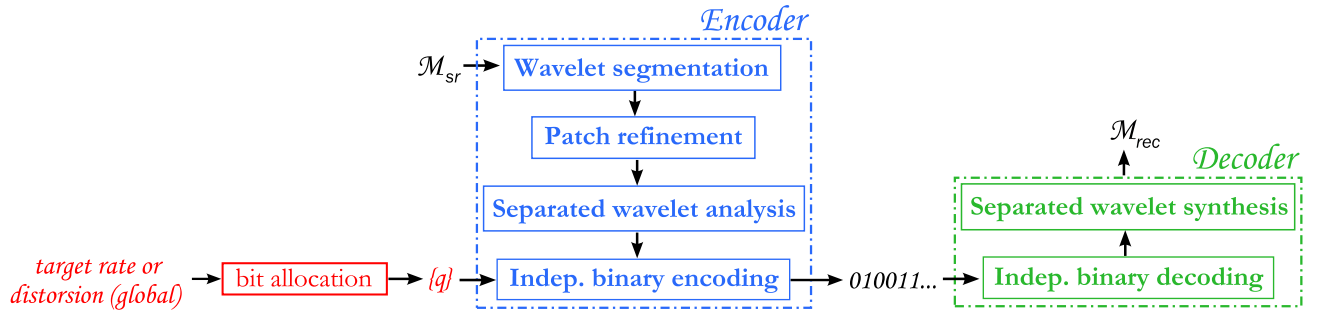
Figure 1. Principal fonctionnalities of our framework which aims at locally encoding a semi-regular mesh M_{sr} in order to propose a robust and efficient reconstruction M_{rec} on the client side.

2.2.4. Semi-regular mesh compression algorithms

The application of the MR analysis on the semi-regular meshes, resulting from these latter algorithms and mainly used for progressive compression purposes, can be based on various subdivision schemes. Most of the existing methods[9, 11, 20, 21] have benefited from interpolating subdivision schemes for the low-resolution versions to be good approximations of the original object (in a least-squares sense). In other words, to provide numerical stability of the fitting operation and have a more stable wavelet construction for practical applications than with approximating schemes.

But other authors[22, 23] have recently proposed a wavelet construction based on the Loop subdivision and the lifting scheme. They have managed to overcome the Khodakovsky[19] filter drawbacks by constructing stable schemes for the wavelet analysis and synthesis with a linear time complexity.

All of these previously described algorithms have applied a global wavelet decomposition, using the same scheme on the entire surface of the mesh. We propose a new framework to improve the latter compression algorithms. It's obvious that for any remeshing algorithm applied on natural objects, the information to be coded (the wavelet coefficients) is heterogeneous all over the surface and mainly depend on the prediction power of the scaling functions. Thus, we propose to partition the mesh so as to analyse it differently to further reduce the compression costs.

3. PROPOSED METHOD

We have introduced the different existing remeshing algorithms that transform an irregular model into a semi-regular one. Semi-regular meshes represent the input models of our framework that aims at detecting the heterogeneity relatively to the wavelet coefficients in order to locally decompose the surface. The principal fonctionnalities of these local analysis and synthesis are presented in Fig. 1 and detailed in the following subsections. The analysis begins with a shape segmentation oriented by the distribution of the wavelet coefficient magnitude and polar angle, followed by a patch refinement for establishing a hierarchical partitioning. Given this structure, an independent wavelet decomposition and coding can be realized, considering some possible optimizations for the binary allocation of each produced partition. On the synthesis side, the last two treatments are reversed to reconstruct an approximation of the initial model.

3.1. Segmentation based on wavelet measures

We present our extension of the segmentation algorithm of Lavoué *et al.*,[7] based on the wavelet coefficient magnitude and polar angle and which can be computed on any mesh of the hierarchy produced by a global decomposition. We first propose to review briefly the computation of the wavelet coefficients, and then the classification and segmentation algorithms.

3.1.1. Wavelet coefficients as a segmentation criterion

The decorrelation power of the wavelets has been trully proven for images and videos, with the standards JPEG-2000 and MPEG, but also for meshes. Appart from the coarser mesh, they represent the only information to code in order to obtain a progressive compression. We propose to study their distribution in all the resolution levels, so as to identify homogeneous regions. More precisely, we are interested in the coefficient magnitude and polar angle, measures that every existing compressing algorithm tend to minimize, while using a common scheme for the whole model. Their distribution can then reveal that for some regions of the mesh, the former prediction scheme is well adapted because the values are close to zero. But usually there remain some regions where another prediction scheme, decomposition or quantization can provide better results in term of compression.

For 3D meshes, the facet refinement of a coarse mesh during the multiresolution synthesis, consists in first applying a canonical quadrisection. This one-to-four triangle construction is based on the addition of three new vertices in the middle of each edge composing the facets of the coarse mesh. The position of these newly added vertices is obtained by the prediction operation, followed by the wavelet coefficient addition. Consequently the common representation of the wavelets consists in associating them with their corresponding coarser model edges. Consequently the measures we consider are linked to the edges of each resolution level, except for the finer representative of the hierarchy. The classification and segmentation algorithms we have adapted were formally designed to partition mesh data associated to vertices, so that even after several adaptations, the best results were obtained with measures associated to vertices. They correspond to the mean of the measures linked to the incident edges.

The wavelet transform used in this study belongs to the class of second-generation wavelets, specially constructed to adapt to irregular point sets and introduced by Sweldens.[24, 25] This construction produces filters with good properties like vanishing moments or orthogonality which is primordial for compression purposes. For a more detailed explanation of the wavelet decomposition construction, the reader is invited to see our previous paper.[26]

Considering the segmentation based on the distribution of the wavelet coefficient magnitude, we have noticed that the smooth parts of a mesh are clearly separated from the rough, textured or noisy ones. It's also well suited for detecting the sharp creases or high curvatures, as the wavelet coefficients represent the high-frequencies lost during the coarsification of the input model.

Moreover the distribution of the polar angle is interesting for distinguishing the coefficients that only have a normal component from those for which the parametric information isn't implicit. The resulting segmentation can then be used by our local wavelet coding framework to adapt the wavelet coefficient representation and coding so as to produce closer results than those obtained by the Normal Mesh compression algorithm. This latter produces actually one of the best compression rates gathering all the high frequency energy in the normal direction, so we have first studied the distribution of the described measurements on objects remeshed with this algorithm.

As the non-lifted butterfly scheme is used on these semi-regular models to produce the best results in term of compression, the corresponding wavelet distribution will be used to further reduce the compression costs. For a comparison, we also have applied our framework on objects remeshed with another famous remeshing algorithms, MAPS,[13] in association with a non-lifted butterfly wavelet analysis. But it can adapt to the specificity of any remeshing algorithm, showing the regions where the produced coefficients could be further reduced.

We present in Fig. 2 to 4 the corresponding distributions for each resolution level of the Rabbit, Venus and Horse models. But as the segmentation algorithm can only be applied on one mesh of the hierarchy, we propose to clusterize all the coefficients in one mesh so as to take into account all the high frequencies lost during the coarsification. For that purpose, we have compared several possible aggregations. Normalizing each coefficient according to its own level extrema values and computing the mean of these values for all the corresponding incident edges of a vertex have given some interesting results as we can see in the last picture of Fig. 2 to 4.

These results have been obtained by applying a Gaussian Normalisation, aiming at not taking into account the extrema values of the interval. This normalization is allowed because the associated histograms (presented in Fig. 2 to 4) have a Gaussian normal distribution. With this assumption, then, about 68% of the values are within one standard deviation of the mean, about 95% of the values are within two standard deviations, and
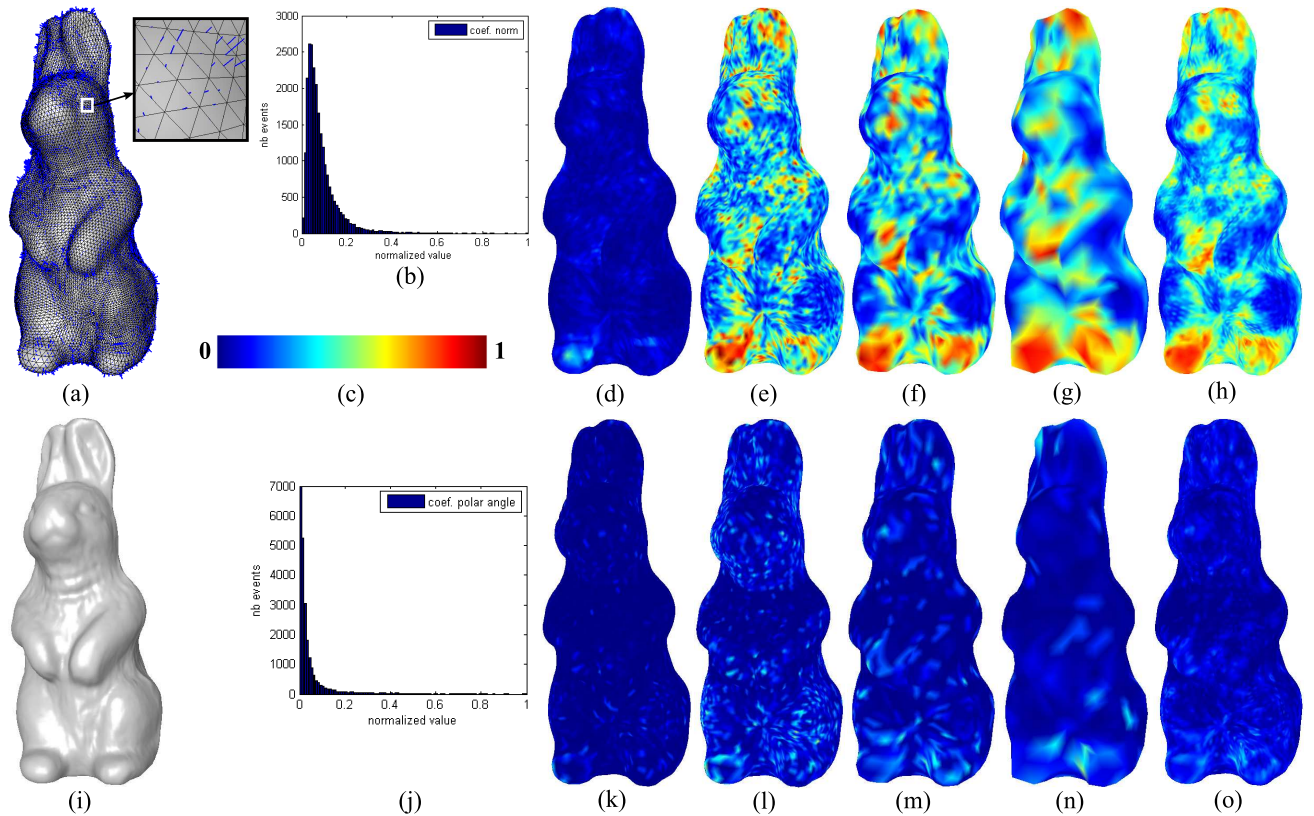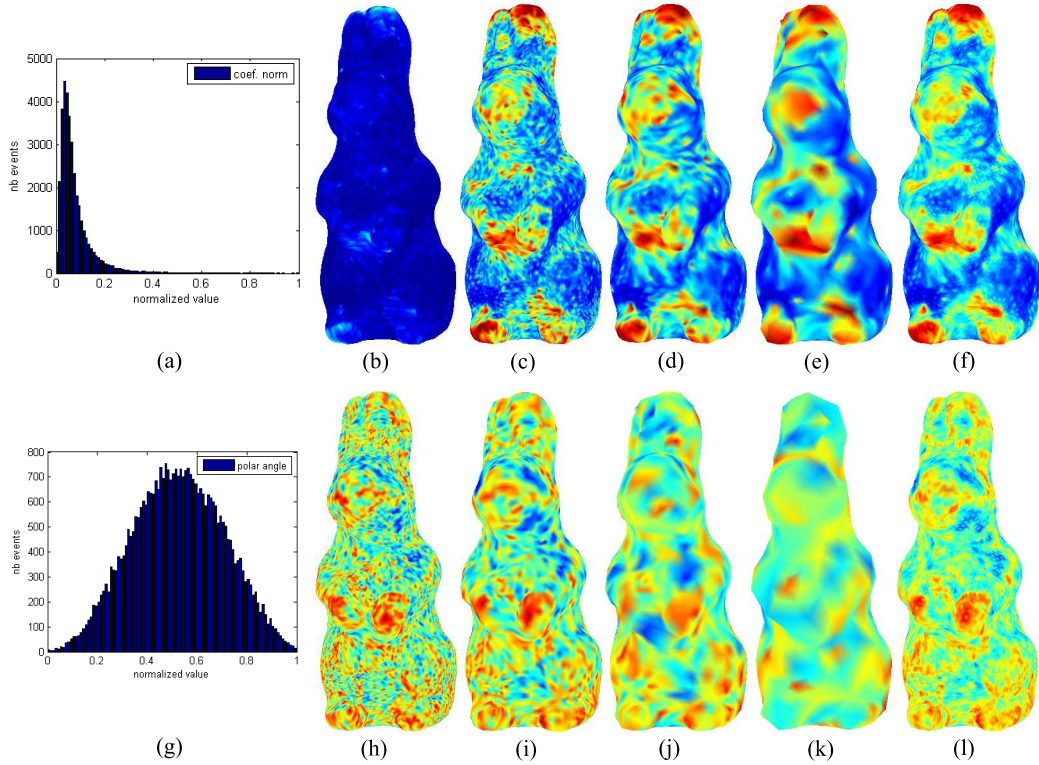
Figure 2. Distribution of the wavelet coefficient magnitude and polar angle on different resolution levels for the Rabbit model. The decomposition has been produced with the non lifted Butterfly scheme on a Normal Mesh. (a) Wavelet coefficients represented as 3D vectors linked to edges of the 1st resolution level (multiplication factor: 20) ; (i) Original model ; (b, j) Histograms of the normalized magnitude and polar angle for the five resolution levels ; (c) Color scale used for the next figures ; (d, k) Distributions of the normalized magnitude and polar angle on the 1st decomposition level ; (e-g, l-n) Same distributions but using a Gaussian Normalisation on the first three levels ; (h, o) Gaussian normalized distribution means computed on the five decompositions and represented on the 1st level.

about 99.7% lie within three standard deviations. This is known as the 68-95-99.7 rule, or the empirical rule, defining the confidence intervals. We have considered the second percentage for all the treatments because it has given sufficiently good results without a more important restriction.

Fig. 2 to 4 show different kinds of wavelet coefficient distributions on several 3D models remeshed by the Normal Mesh and MAPS algorithms. For each mesh, the Gaussian normalized distribution mean of all the wavelet coefficients (represented in the last column) has given the best results when considering a classification and segmentation based on the wavelets. More particularly, the last raw of Fig. 2 shows that the coefficient polar angle distribution obtained on a Normal Mesh is not enough revealing for applying a classification, even after a Gaussian Normalisation. We only present it on the Rabbit model, but it can be generalized for the other meshes. As we can deduce from the histogram, the quasi totality of the wavelet coefficients obtained after this remeshing lie along the surface normal. This is not the case when dealing with the MAPS remeshed models, as illustrated by the last raw of Fig. 3.

On globally smooth models, the coefficient magnitude distribution allows to identify the high curvatures characterizing the eyes, ears, feet or the nose of the Rabbit and Horse models. This distribution emphasizes also the textured parts, such as the hair of the Venus head.

Figure 3. Distribution of the wavelet coefficient magnitude and polar angle on different resolution levels for the Rabbit model remeshed by MAPS. The decomposition has been produced with the non lifted Butterfly scheme. (a, g) Histograms of the normalized magnitude and polar angle for the five resolution levels ; (b, h) Distributions of the normalized magnitude and polar angle on the 1st decomposition level ; (c-e, i-k) Same distributions but using a Gaussian Normalisation on the first three levels ; (f, l) Gaussian normalized magnitude means computed on the five decompositions and represented on the 1st level.

3.1.2. Mesh classification and segmentation steps

Our algorithm uses the distribution of the wavelet measures (associated to the simplices of the mesh) in association with an adaptation of the classification and segmentation algorithms of Lavoué *et al.*[27] They exploit the principal curvature values computed in each vertex using the estimation of the curvature tensors defined by Cohen-Steiner and Morvan.[28] Our adaptation produces connex regions that share homogeneity relatively to the information used to progressively compress a mesh. For more details on the adaptation of this algorithm, the reader is invited to consult our preceding paper.[26]

The classification algorithm of Lavoué *et al.*[7] was first used to create two groups of vertices, one with the smallest measure amplitudes and the other with the highest ones. We present the results obtained for the coefficient magnitude and polar angle separated classifications, in order to emphasize the differences between the two remeshing algorithms we have considered. But it is also possible to associate these measures.

The construction of the connex partitions, using the region growing and merging algorithms, consists in transmitting the studied measure from vertices to triangles, starting from seed triangles having their three vertices on the same cluster. The region merging algorithm mainly aims at reducing the oversegmentation resulting from the growing step, thanks to a region adjacency graph. The graph reduction stops when the smallest edge is larger than a given threshold. This reduction is based on the similarity distance D_{ij} which gather studied measure similarities, size and common perimeter of the two regions.

Thanks to this framework, a mesh decomposition in a finite number of regions can be created at a given resolution level, as we can see in Fig. 5 to 8 for the preceding models. In order to take into account a maximum
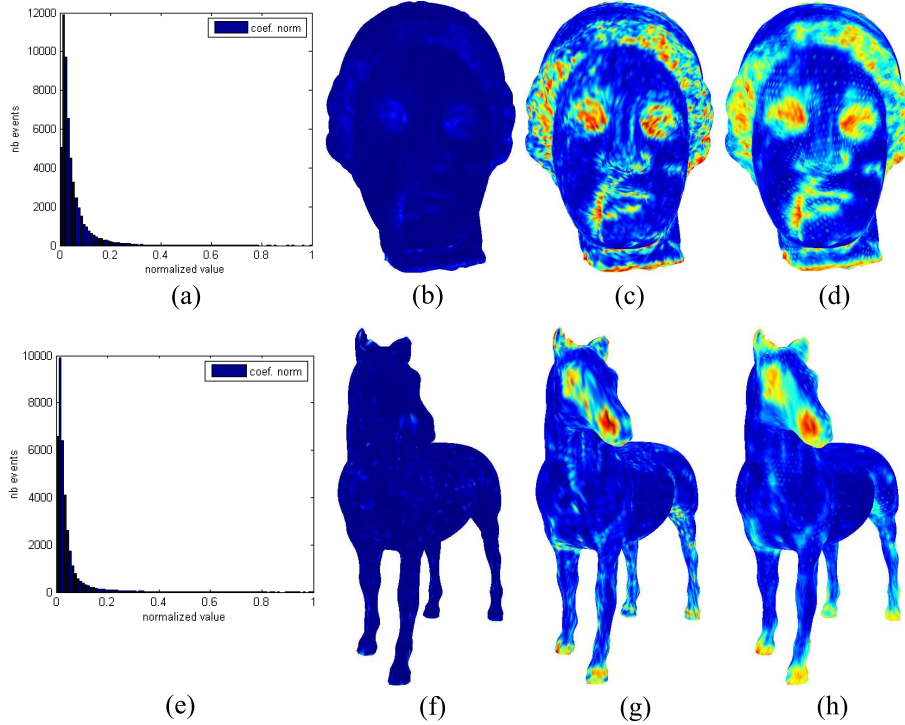
Figure 4. Distribution of the wavelet coefficient magnitude on the Venus and Horse models remeshed by the Normal Mesh algorithm. The decomposition has been produced with the non lifted Butterfly scheme. (a, e) Histograms of the normalized coefficient magnitude for all the resolution levels ; (b, f) Distributions of the normalized coefficient magnitude on the 1st decomposition level ; (c, g) Same distributions but using a Gaussian Normalisation on the 1st level ; (d, h) Distribution means of all the Gaussian normalized magnitudes on the 1st level.

number of the wavelet coefficients computed on the surface, we have always considered the segmentation of the first decomposition level distribution mean of all the Gaussian normalized coefficients. These distributions are reported in the first pictures of Fig. 5 to 8, followed by the two-clustered classification of the vertices. The face oriented classification presented in the third column is the result of the application of the region growing and merging stages. The colors used for the clusters are randomly chosen. The different classifications obtained on the Rabbit model and presented in Fig. 5 and 6, always emphasize the characteristic parts of the mesh delimited by high curvatures (ears, feet and nose) but the coefficient magnitude seems more appropriate to separate the textured neck or the eyes from the smoother surroundings. The same kinds of observations have been made on the two other models.

Since our goal consists in analysing independently each patch with a special subdivision schemes or quantization, we need to be able to apply a separate multiresolution analysis in each produced partition. We present in the next subsection the method we have considered and comment on the rest of the pictures.

3.2. Local multiresolution analysis computed on connex partitions

In order to analyse, quantify and encode separately each connex region, we need to be able to decompose independently each one into several levels. Consequently, we have chosen to start from the level on which the segmentation was produced and to coarsen it so as to obtain good approximations of the former partitions on the coarser meshes. The final stage consists in projecting back the approximations on the finest model (the original one), in order to begin the local analysis.
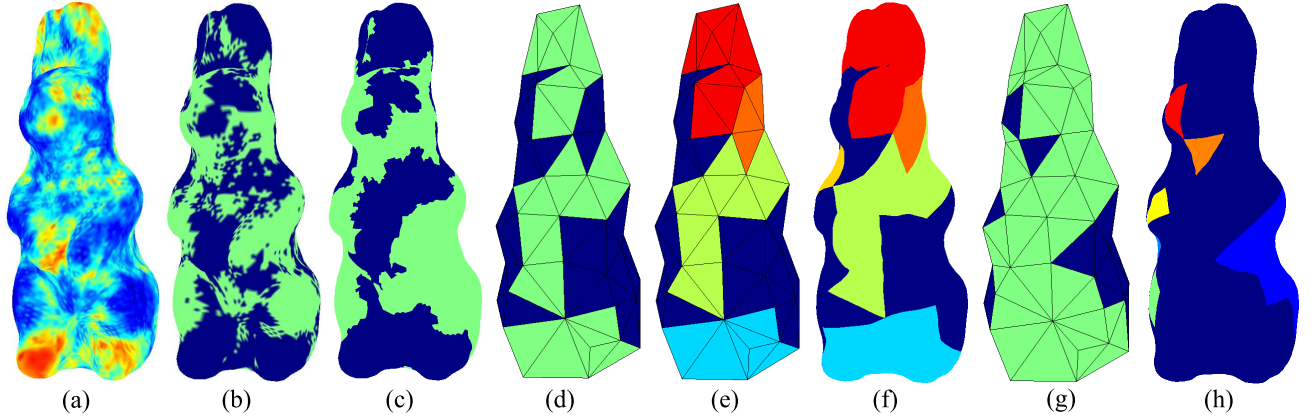
Figure 5. Classification and segmentation based on the coefficient magnitude for the Rabbit model, remeshed by the Normal Mesh algorithm. (a) Distribution mean of all the Gaussian normalized coefficient magnitudes on the 1st level ; (b) Two-clustered classification on the same level ; (c) Same classification after the region merging step ; (d, g) Cluster projections on the coarsest (5th) level using the two different rules and (e) the first projection rule corresponding connex regions ; (f, h) Connex partitions projected on the finer mesh.

3.2.1. Determination of the coarsest acceptable model for the segmentation projection

One of our contributions is the projection of the fine classification and segmentation on the coarser resolution levels. If we assume that the segmentation was computed on the resolution level n, the projection will start on the immediately coarser model (level $n + 1$) and will continue until the produced regions are too far away from the initial ones. Experimentally, we have noticed that it generally occurs when the coarse mesh number of triangles is smaller than 130. That's why we have projected the partitioning until the 5th resolution level for all the considered models.

We have used two different rules to determine for each coarse triangle (represented by t in Fig. 9), its cluster affiliation, according to its incident four finer facets. For the first rule, if at least three of the four fine triangles belong to a given cluster, the corresponding coarser triangle will also belong to this cluster. The projection using this rule is illustrated in Fig. 10. If an equality occurs, we have the choice to favour one of the two clusters, depending on the final stake. We have chosen to favour the non smooth cluster (represented in green in Fig. 10) because one of our goal is to show the reconstruction produced when any wavelet is associated to the smooth parts. Following this latter objective, we have also proposed a second rule that always favour the non smooth cluster if at least one of the four fine triangles are not smooth.

The cluster and partitioning coarse projections are presented in Fig. 5 to 8 for the first or both rules. For every cluster projection, the blue color is associated to the smooth cluster. We can see that the first rule has produced projections which are not really far from the former ones. The results obtained with the second rule are much more differents, except for the Horse model which is predominantly composed of smooth parts.

The last stage consists in projecting back the coarse segmentation on the finest mesh (the original one), so as to be able to compute a local multiresolution analysis considering different treatments on each partition.

3.3. Separated wavelet analysis

Once the projection on the finest level is realized, we can decompose each partition until the coarsest acceptable level (the 5th one). This patch-independent analysis can be based on each partition cluster type, in order to differentiate the treatments on smooth and high frequency parts. It produces as much "wavelet files" as the number of created regions that can be separetely quantified and entropy coded.

Considering the wavelets to produce such a hierarchy, we aim at finding the best prediction scheme for each specificity in the surface, in order to improve the rate/distorsion (r/d) results in comparison with the global
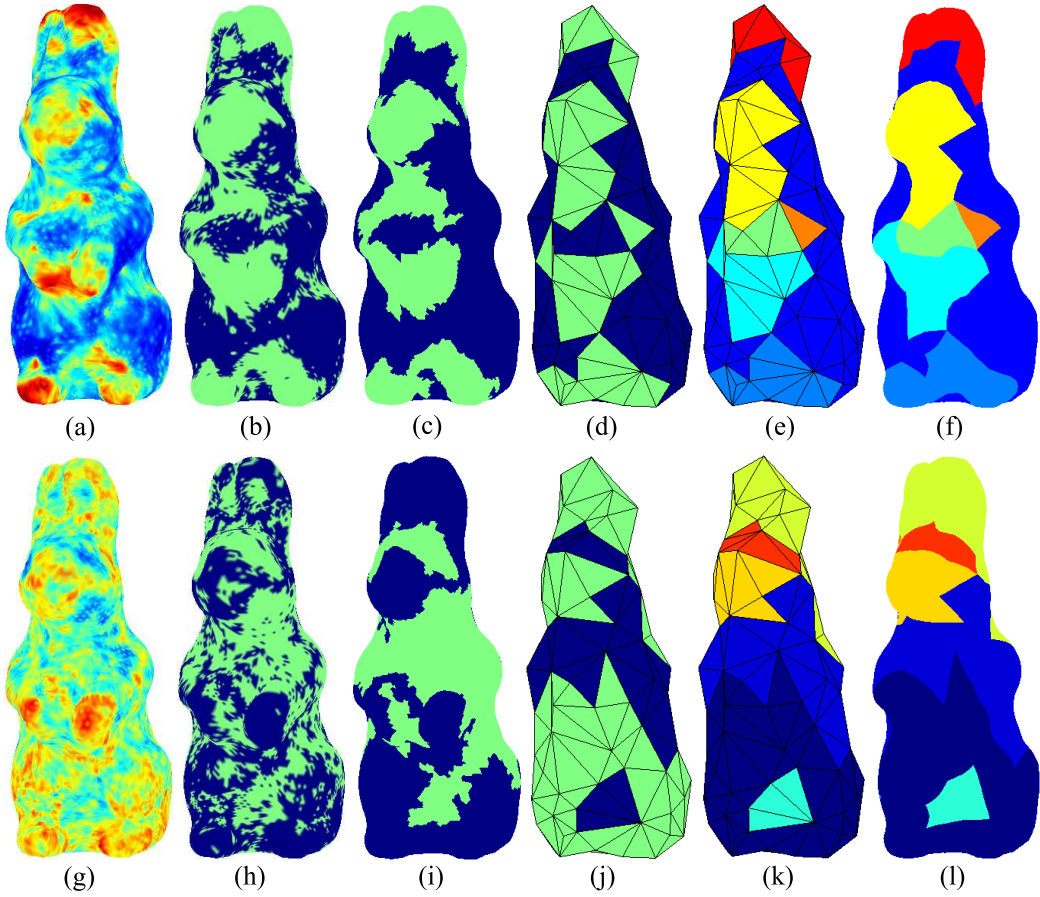
Figure 6. Classification and segmentation based on the coefficient magnitude and polar angle for the Rabbit model, remeshed by MAPS. (a, g) Distribution means of all the Gaussian normalized magnitudes and polar angles on the 1st level ; (b, h) Two-clustered classifications on the same level ; (c, i) Previous classifications refined by the region merging step ; (d, j) Cluster projections using the first rule, on the coarsest (5th) level and (e, k) the corresponding connex regions ; (f, l) The same partitions projected on the finer mesh.
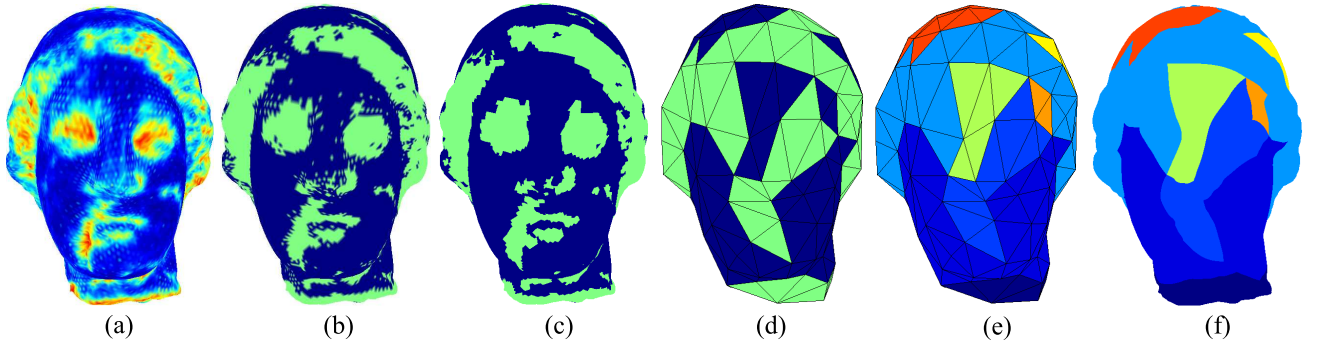

Figure 7. Classification and segmentation based on the coefficient magnitude for the Venus model, remeshed by the Normal Mesh algorithm. (a) Distribution mean of all the Gaussian normalized coefficient magnitudes on the 1st level ; (b) Two-clustered classification on the same level ; (c) Same classification after the region merging step ; (d) Cluster projection using the first rule on the 5th level and (e) the corresponding eleven created connex regions ; (f) Previous partitions projected on the finer mesh.
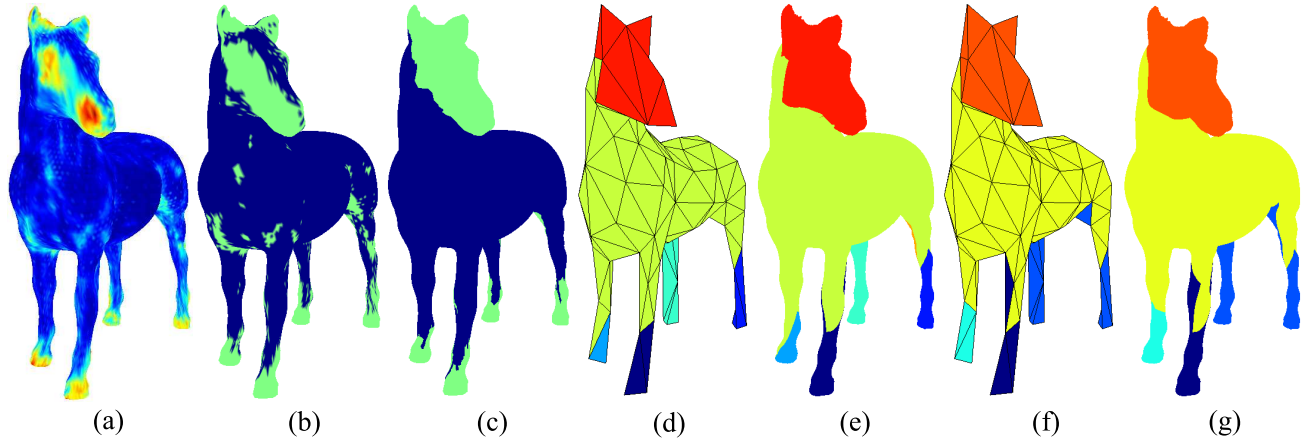
Figure 8. Classification and segmentation based on the coefficient magnitude for the Horse model, remeshed by the Normal Mesh algorithm. (a) Distribution mean of all the Gaussian normalized coefficient magnitudes on the 1st level ; (b) Two-clustered classification on the same level ; (c) Same classification after the region merging step ; (d, f) Corresponding partition projections using the two different rules, on the 5th level ; (f) Previous connex regions projected on the finer mesh.
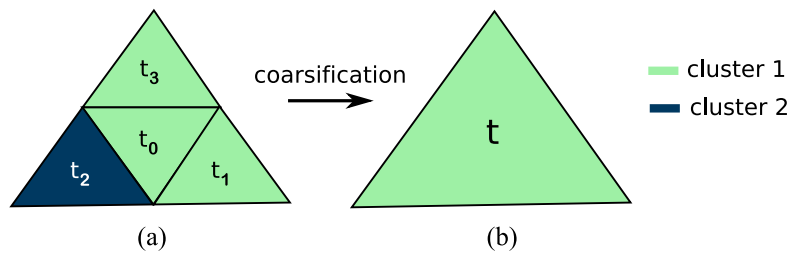
Figure 9. Example of the coarse facet cluster affiliation determination (b) according to its incident four finer facets (a).
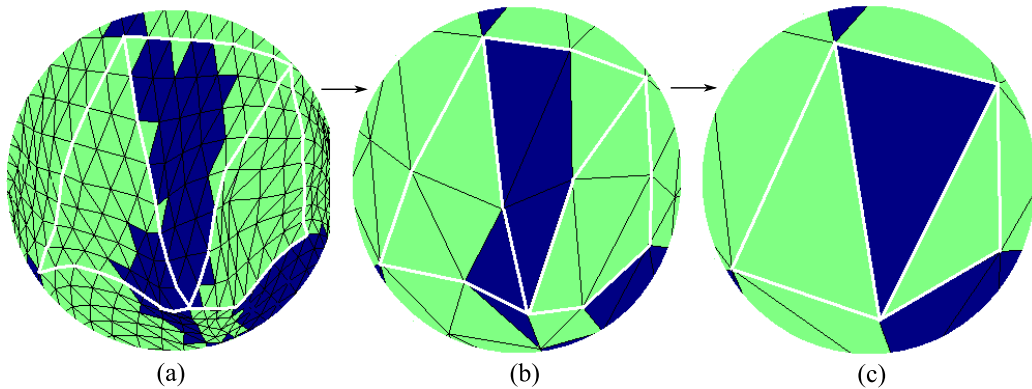
Figure 10. Example of the coarse facet cluster affiliation after two successive coarsifications with our first rule. Using our second rule, if we consider that the "smooth triangles" are represented in blue, the final three coarse triangles would have been identified rough (in green).

12

treatment. We illustrate this consideration in the next section on a synthetic object. For the other models, another kind of treatment can also be considered which is discussed in the conclusion.

3.4. Zerotree coding and binary allocation

The most powerfull compression algorithms for this kind of 3D representations use the geometric wavelets on semi-regular meshes. The coefficients are hence quantized and compressed with a very efficient method, based on their distribution in the resulting hierarchy (zerotree representation) or considering the neighbouring coefficients (spatial correlation). A scalar quantization is generally used, so we are faced with three independent coders. Finally, an arithmetic coding is added to further compress the data.

For the coefficient compression, we have first considered the same zerotree coding as the one used by Khodakovsky et al.[19] This latter uses an adapted quadtree definition for meshes compared to the algorithm of Said and Pearlman,[29] formerly implemented for images. Their coding exploits the parent-child coefficient correlations, minimizing the significant bits to code at each step. It is also conceived so as to send the highest order bits of the largest magnitude coefficients first, in order to obtain for each bitrate, the best reconstructed model producing the smallest distortion.

Appart from the wavelets, the compression file size also includes the scale coefficients corresponding to the encoding of the coarsest mesh. We have used the embedded coarsest geometry encoding method of Khodakovsky et al.,[19] where the coarsest geometry is stored with the zerotree representation. The connectivity is compressed with a single rate coder, such as the Touma and Gotsman[30] one we have used. Consequently the r/d results consider all these coding treatments.

This data flow is now ready to be transmitted on the network and reconstructed on the client side. All the analysis stages we have described need to be reversed on the decoder side. For a brief recalling, the reader is invited to refer to Fig. 11.

4. EXPERIMENTAL RESULTS AND APPLICATIONS

We present in this section the experimental results we have obtained with our application implemented in C++. It uses the Computational Geometry Algorithm Library (CGAL)[31] and more specifically the polyhedral surface package.

There are lots of applications where the redundancy caused by the partitioned analysis could be a benefit, such as error-resilient coding or watermarking. In order to evaluate this additive information, we first present a comparison between our local MR framework and the global one for the usual 3D models. Then, in order to validate our expectations, we have applied different decomposition treatments on a simple synthetic object, after its segmentation. The r/d improvements we have obtained emphasize that a well adapted decomposition can counterbalance the redundant information added by our local analysis. Finally, we show some other possible applications of our framework.

## 4.1. Magnitude order of the local analysis additional information

Fig. 12 shows the different r/d curves for the preceding 3D objects. $PSNR = 20 \log_{10} peak/d$ where $peak$ is the bounding box diagonal and d the L^2 relative error, corresponding to the following L^2 distance $d(X,Y)$ between the surfaces X and Y :

$$d(X,Y) = \big(\frac{1}{area(X)} \int_{x \in X} d(x,T)^2 dx\big)^{\frac{1}{2}}.$$

This distance was computed with the MESH tool[32] which symmetrized it by taking the max of $d(X,Y)$ and $d(Y,X)$. The rate is reported in bits per irregular vertex (b/v) according to the number of vertices in the original input mesh. We can see the amount of the additive information necessary for the local analysis compared with the global one, using the two different projection rules and a common treatment for all the regions of the surface. The associated number of created regions for both rules and the percentage of the identified clusters are reported in Table 1, for a better understanding of the curves.
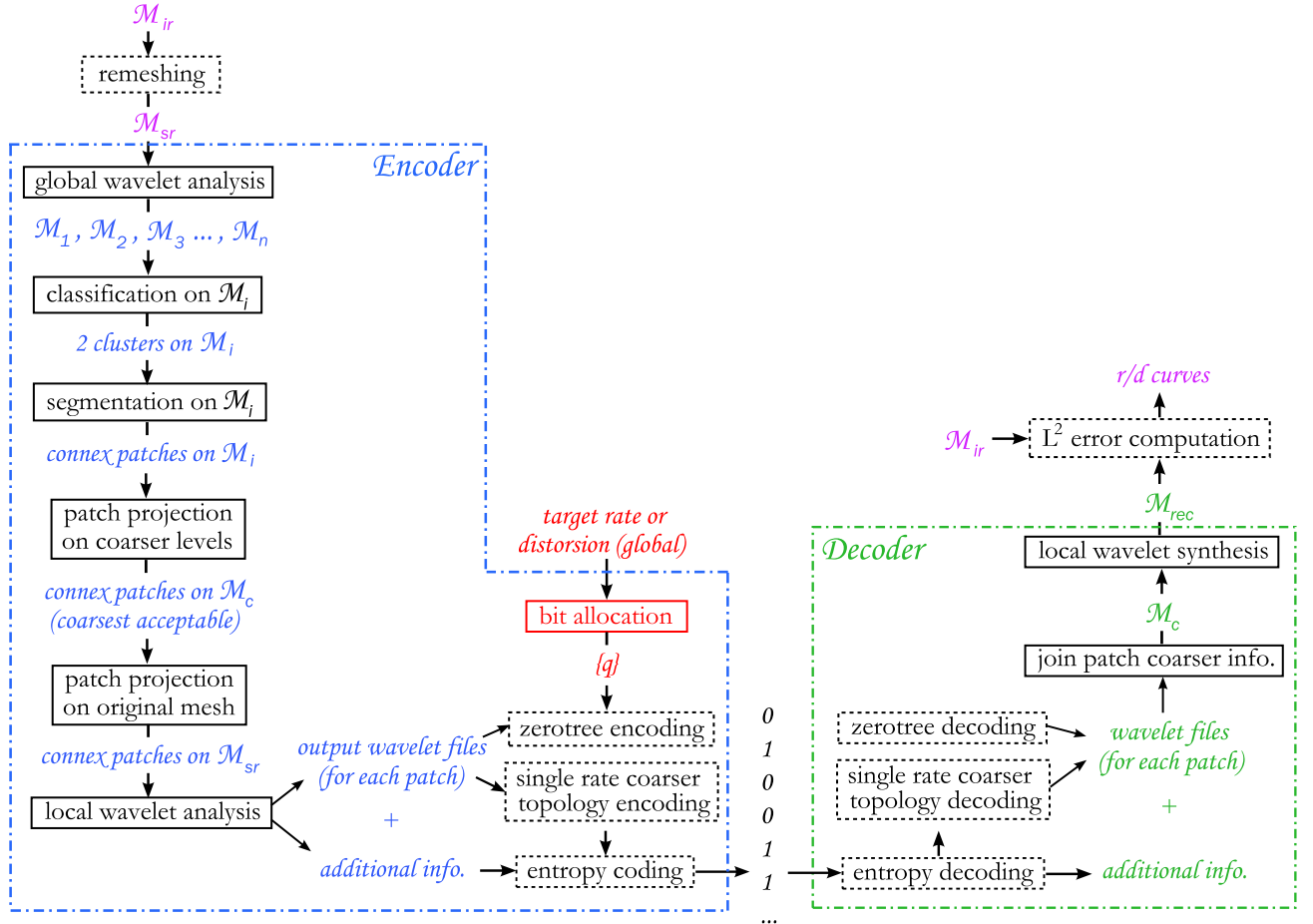
Figure 11. Steps involved during the local wavelet analysis and synthesis. The analysis begins with a semi-regular mesh M_{sr} obtained by applying a remeshing algorithm on an original irregular mesh M_{ir}. Then a global wavelet analysis decomposes the semi-regular model into n coarser meshes $M_1, M_2, ...M_n$. Then we can choose any of these produced levels M_i to apply the classification and segmentation steps. To compress independently each constructed region, we finally propose to project them on the coarser resolution levels before separating them and applying the zerotree and entropy coding. On the synthesis side, the coarsest patches are first glued followed by the addition of the decompressed wavelet, to form the reconstructed object M_{rec} that is compared to the original one, so as to evaluate our method.
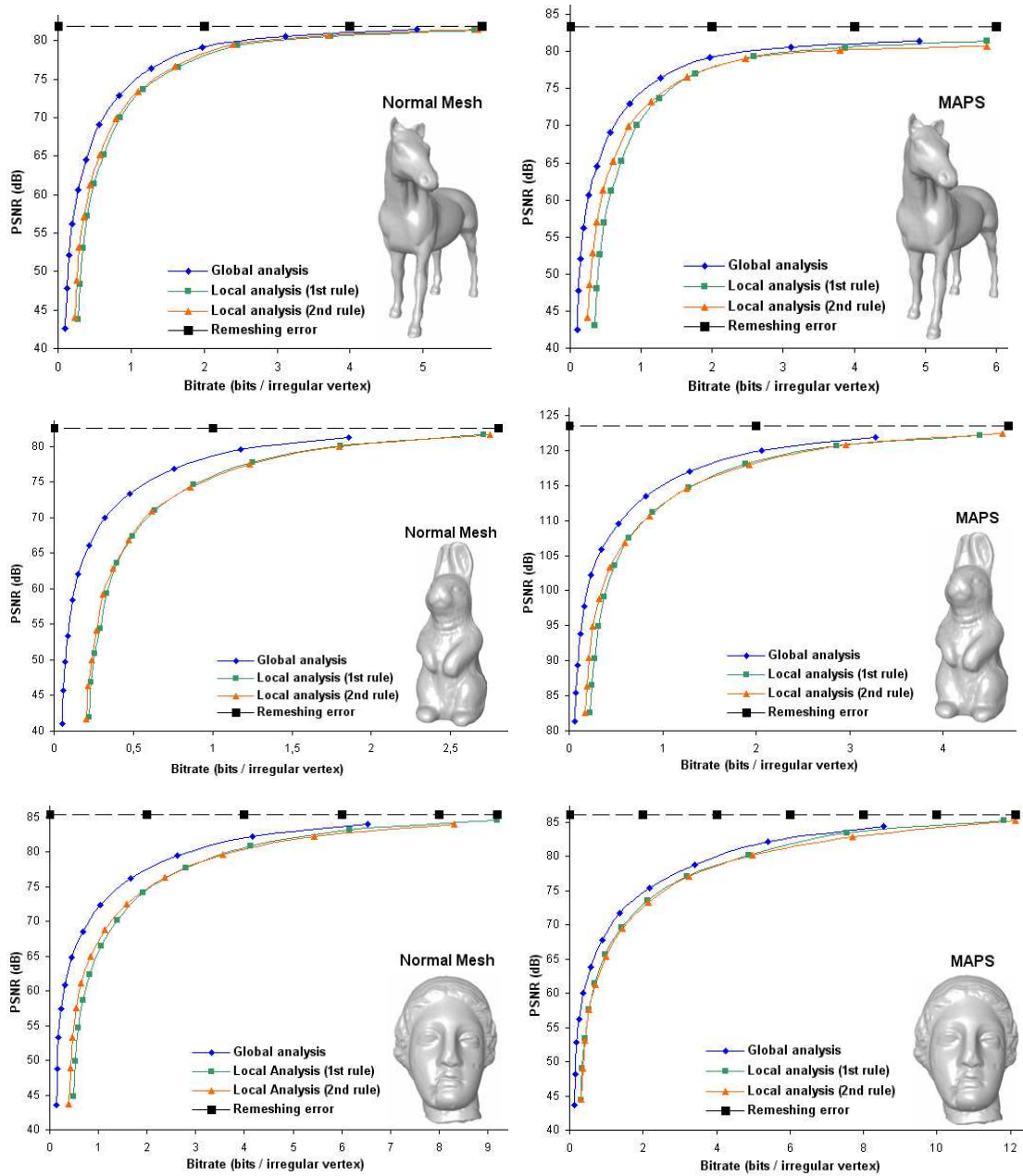
Figure 12. Rate-distortion curves for the usual 3D models remeshed by the Normal Mesh algorithm. The shape partitions used for the local wavelet analysis and synthesis are based on the wavelet coefficient magnitude.

Table 1. Segmentation characteristics based on the wavelet coeffcient magnitude for the usual models. The number of created regions and rough cluster percentages are associated to the coarse projection using the two different rules.

	# vtx	# face	# reg. (1st rule)	% rough	# reg. (2nd rule)	% rough
Rabbit Normal	70,758	141,312	9	29%	8	63%
Rabbit MAPS	67,039	134,074	8	22%	5	49%
Horse Normal	112,642	225,280	7	25%	5	37%
Horse MAPS	112,642	225,280	10	24%	6	35%
Venus Normal	163,842	327,680	11	43%	9	78%
Venus MAPS	163,842	327,680	6	19%	6	38%
Feline Normal	258,046	516,096	10	39%	8	56%

The additional cost produced by our local framework when using the same treatment on each partition can be evaluated to 3 or 4 dB in average compared to the global treatment, for a bitrate greater than 0.5 b/v. Moreover, the partitions constructed with our second rule projection have given better r/d results with this kind of analysis, because of the smaller number of created regions which implies less redundant information to encode. The section 4.3 demonstrates also its superiority for a special type of reconstruction.

The redundancy introduced by the partitioning can be compensated by a well adapted method on each region. For the smooth ones, the prediction produced by the Butterfly subdivision scheme appears really accurate because the wavelet coefficients are close to zero. For the other regions, higher details are generally needed to represent the high frequencies.

This information, which greatly contributes to the visual realism of the reconstructued objects, could be reduced by considering the statistical distribution of the wavelets. Consequently instead of transmitting all the coefficients, some critical statistical elements can be sufficient to regenerate a surface with the same visual aspects and high frequencies. We keep this outlook for future work, considering the work done by Golovinskiy et al.[33] They have developed a statistical model for the analysis and synthesis of facial geometry details so as to improve the 3D face model realism. Moreover, Nguyen et al.[34] have implemented a hole filling algorithm for polygonal meshes that synthesize details based on the close existing geometry. Associated with a determination of the required details needed for an accurate reconstruction, this approach could allow to reduce the wavelet amount.

4.2. Global vs Local wavelet analysis with different schemes on a synthetic object

In order to study the compression behaviour when applying different treatments on the segmented regions, we first wanted to test the application of distinct prediction schemes on a synthesized model. This model, represented in the picture (b) of Fig. 13, has been conceived by applying four successive subdivisions on the coarse mesh illustrated in the picture (a) of Fig. 13, with little additional white uniform Gaussian noise. Our aim was to produce a nearly flat part as opposed to another quasi smoothed region. The following results show that the flat region can be better predicted with the simple midpoint scheme, whereas a "smooth prediction" is more suitable for the other part. This treatment can be realized thanks to the prior segmentation, illustrated in Fig. 13, picture (e). Fig. 14 present the r/d curves associated to the local and global analysis where the bitrate is computed in bits per semi-regular vertex. The improvements in coding performance are obvious for bitrates up to 2 bits/vertex.

4.3. Examples of other possible applications

We finally present some of the other possible applications of our framework.

First of all, if the user is not interested in visualizing a given region, we can only send him or her the coarsest mesh information without the wavelets. Moreover, for the identified smoothed regions, the wavelets are generally not needed for objects visualized on low resolution screens.
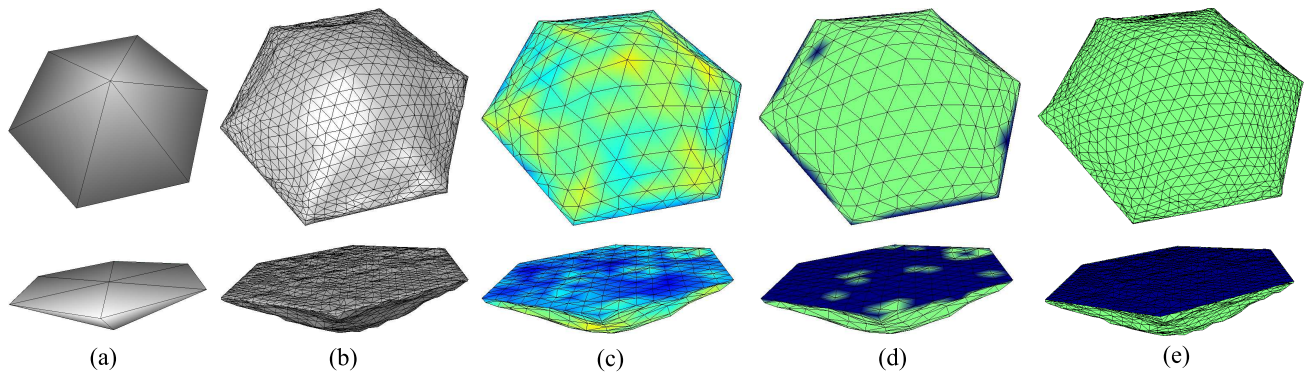
Figure 13. Segmentation of a synthesized model (b) produced by applying four canonical subdivisions on the (a) polyhedron, followed by an additional white uniform Gaussian noise ; (c) Distribution mean of all the Gaussian normalized coefficient magnitudes on the 1st resolution level, using the midpoint scheme ; (d) Two-clustered first classification on the same level ; (e) Final classification after the region merging step.
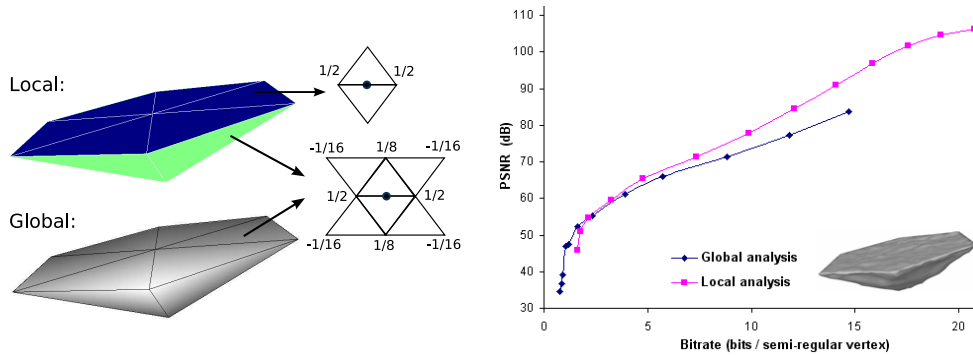
Figure 14. Comparison of the r/d curves obtained with the global and local wavelet analysis (right). The left part emphasizes the possibility of using different prediction schemes when compressing the object with the local framework.

Fig. 15 present different possible reconstructions which have been produced considering the maximal bitrate. For each one, we have specified the corresponding compressed file size in bytes and the L^2 error in units of 10^{-4}. The first column illustrate the result obtained with the global synthesis, whereas the other reconstructions have been produced by our segmentation framework, without considering the wavelets on the smooth partitions. The second and fifth columns present the two classifications used to produce the following reconstructions. They were obtained with the application of our different projection rules.

The first observation is that the single subdivision applied on the smooth regions produces good reconstructions with a lower L^2 error than without subdividing at all. More specifically, for the Horse model, with approximately twice fewer bytes, we obtain a good reconstruction of the Horse model which preserves the important characteristics of the object. This decompression can be sufficient for a visualization on a low resolution device. The Feline model is also well reconstructed with our two local rules, but the file size reduction is less important because it contains a more important percentage of non smooth parts. Finally, the weaker file size gain obtained for the Rabbit mesh can be explained by the more important redundancy induced by the shape of the mesh.

Such as the work published recently by Cheng et al.,[35] we propose a part-based mesh reconstruction with different focuses depending on the user's waiting. Our method can decode perfectly the full details of a meaningfull part, without doing it for other patches. Moreover we obtain a better rendering for the identified "non meaningfull" regions using the subdivision surfaces.

Another interesting application which can benefit from our framework are the error-resilient mesh coding techniques. In this context, Park et al.[36] have recently proposed a two-step partitioning scheme to prevent from the reconstructed mesh degradations encountered when transmission errors occur. As the majority of the coding methods uses a redundancy reduction for providing the most compact bitstreams, the information becomes more sensitive to transmission errors.

Yan et al.[37] had previously considered this issue, but had encountered reconstruction problems because their method could not guarantee a uniform partitioning. For this reason, Park et al.[36] have proposed a shape decomposition into smooth and detailed regions, followed by an additional division into smaller parts to provide partitions of uniform sizes and overcome the latter problems. Moreover, they have observed that the smoothness uniformity within each partition has facilitated the faithful concealment of erroneous partitions. Consequently we could consider to further decompose our patches so as to propose the same kind of algorithm.

5. CONCLUSIONS AND FUTURE WORK

We have presented a new MR analysis local decomposition based on a segmentation of semi-regular meshes according to their surface smoothness. The main contribution of this work is the development of a framework that provide the possibility to apply different coding treatments on specific identified regions, to reduce the compression costs. This compression oriented framework is applicable to any semi-regular polyhedral surface. We have demonstrated on a synthesized 3D model that the produced redundancy can be compensated by a well adapted treatment on each analysed region.

Consequently the first perspective of this work is to adapt a statistical analysis and synthesis model for the non smooth partitions to be decomposed differently, in order to produce better r/d results than with a unique scheme on the entire surface. A possible issue could consist in collecting only the critical elements to regenerate the same visual aspects and high frequencies of the studied surface.

The r/d results presented in this work for the local analysis could also be improved considering a rate-distortion optimization. Following the work done by Payan et al.,[38] we would like to further optimize the wavelet quantization and bit allocation for each produced patch, with respect to its distortion contribution on the entire surface. Their bit allocation process minimizes the reconstruction error for a given bit budget, with an error-driven wavelet coefficient quantization and improves the coding performance up to +2.5 dB compared to the original zerotree coder of Khodakovsky et al.[19] Consequently we propose to predict the optimized quantization for each patch with the same kind of model-based approach Payan et al.[38] and Parisot et al.[39] have used.
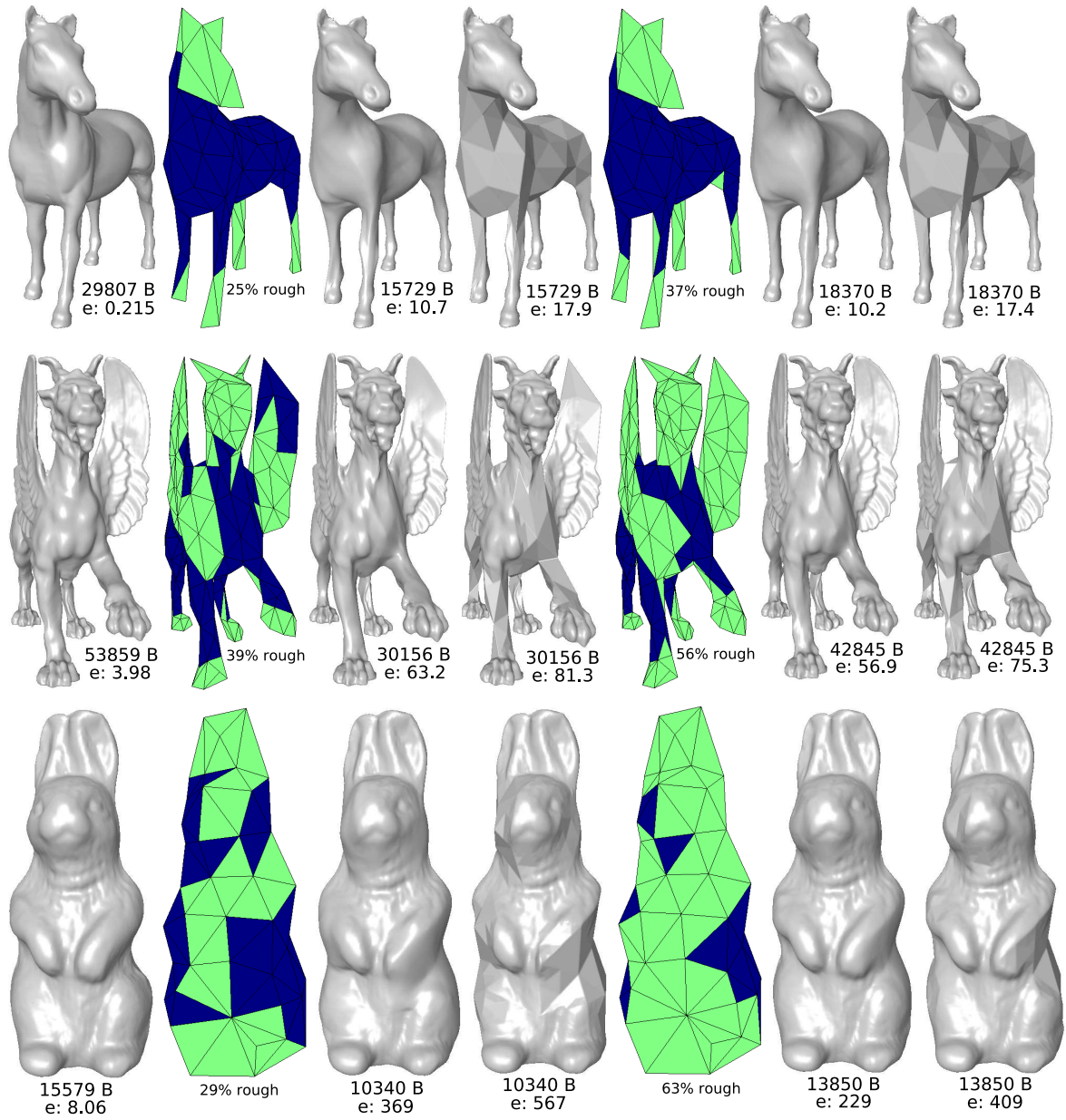
Figure 15. The possible reconstructions with our flexible local framework and considering the maximal bitrates. 1st column: reconstructions obtained from a global wavelet decomposition ; 2nd & 5th column: two-clustered classifications using the two different rules and projected on the 5th level (smooth cluster in blue) ; 3rd & 6th column: reconstructions produced with the non lifted Butterfly subdivision, followed by the wavelet addition in the non smooth parts ; 4th & 7th column: same reconstructions but without any subdivision in the smooth parts. We have reported the corresponding coding file size in bytes and L^2 error in units of 10^{-4} for each considered reconstruction.

Finally, we could also improve the produced regions, using a different method associated to a remeshing stage. Given the former partitioning on the 1st resolution level, it could be decimated and remeshed, considering the surface anisotropy such as the work proposed by Alliez *et al.*[40]

ACKNOWLEDGMENTS

REFERENCES

1. M. Attene, S. Katz, M. Mortara, G. Patane, M. Spagnuolo, and A. Tal, "Mesh segmentation - a comparative study," in *SMI '06: Proceedings of the IEEE International Conference on Shape Modeling and Applications 2006 (SMI'06)*, p. 7, IEEE Computer Society, (Washington, DC, USA), 2006.

2. M. Garland, A. Willmott, and P. S. Heckbert, "Hierarchical face clustering on polygonal surfaces," in *SI3D '01: Proceedings of the 2001 symposium on Interactive 3D graphics*, pp. 49–58, ACM Press, (New York, NY, USA), 2001.

3. D. Cohen-Steiner, P. Alliez, and M. Desbrun, "Variational shape approximation," *ACM Trans. Graph.* **23**(3), pp. 905–914, 2004.

4. A. P. Mangan and R. T. Whitaker, "Partitioning 3D surface meshes using watershed segmentation," *IEEE Transactions on Visualization and Computer Graphics* **5**, pp. 308–321, October/December 1999.

5. Y. Sun, D. Page, and J. Paik, "Triangle mesh-based edge detection and its application to surface segmentation and adaptive surface smoothing," in *IEEE International Conference on Image Processing*, **3**, pp. 825–28, (Rochester, NY, USA), 2002.

6. A. Razdan and M. Bae, "A hybrid approach to feature segmentation of triangle meshes," *Computer-Aided Design* **35**(9), pp. 783–789, 2003.

7. G. Lavoué, F. Dupont, and A. Baskurt, "Curvature tensor based triangle mesh segmentation with boundary rectification," in *Computer Graphics International*, pp. 10–17, 2004.

8. A. Gersho and R. M. Gray, *Vector quantization and signal compression*, Kluwer Academic Publishers, Norwell, MA, USA, 1991.

9. M. Lounsbery, T. D. DeRose, and J. Warren, "Multiresolution analysis for surfaces of arbitrary topological type," *ACM Transactions on Graphics* **16**(1), pp. 34–73, 1997.

10. M. Eck, T. DeRose, T. Duchamp, H. Hoppe, M. Lounsbery, and W. Stuetzle, "Multiresolution analysis of arbitrary meshes," in *SIGGRAPH '95: Proceedings of the 22nd annual conference on Computer graphics and interactive techniques*, pp. 173–182, (New York, NY, USA), 1995.

11. P. Gioia, "Reducing the number of wavelet coefficients by geometric partitioning," *Comput. Geom. Theory Appl.* **14**(1-3), pp. 25–48, 1999.

12. I. Guskov, "Manifold-based approach to semi-regular remeshing," *Graph. Models* **69**(1), pp. 1–18, 2007.

13. A. W. F. Lee, W. Sweldens, P. Schröder, L. Cowsar, and D. Dobkin, "Maps: Multiresolution adaptive parameterization of surfaces," *Computer Graphics* **32**(Annual Conference Series), pp. 95–104, 1998.

14. C. T. Loop, "Smooth subdivision surfaces based on triangles," 1987.

15. I. Guskov, K. Vidimce, W. Sweldens, and P. Schröder, "Normal meshes," in *Siggraph 2000, Computer Graphics Proceedings*, pp. 95–102, 2000.

16. J.-H. Yang, C.-S. Kim, and S.-U. Lee, "Semi-regular representation and progressive compression of 3-d dynamic mesh sequences," *IEEE Transactions on Image Processing* **15**(9), pp. 2531–2544, 2006.

17. A. Khodakovsky, N. Litke, and P. Schröder, "Globally smooth parameterizations with low distortion," *ACM Trans. Graph.* **22**(3), pp. 350–357, 2003.

18. N. Ray, W. C. Li, B. Levy, A. Sheffer, and P. Alliez, "Periodic global parameterization," tech. rep., Jan. 2005.

19. A. Khodakovsky, P. Schröder, and W. Sweldens, "Progressive geometry compression," in *Siggraph 2000, Computer Graphics Proceedings*, pp. 271–278, 2000.

20. A. Khodakovsky and I. Guskov, "Compression of normal meshes," in *Geometric Modeling for Scientific Visualization. Springer-Verlag*, 2003.

21. F. Payan and M. Antonini, "Mean square error approximation for wavelet-based semiregular mesh compression," *Transactions on Visualization and Computer Graphics (TVCG)* **12**, July/August 2006.

22. M. Bertram, "Biorthogonal loop-subdivision wavelets," *Computing* **72**(1-2), pp. 29–39, 2004.

23. D. Li, K. Qin, and H. Sun, "Unlifted loop subdivision wavelets," in *PG '04: Proceedings of the Computer Graphics and Applications, 12th Pacific Conference on (PG'04)*, pp. 25–33, IEEE Computer Society, (Washington, DC, USA), 2004.

24. W. Sweldens, "The lifting scheme: A new philosophy in biorthogonal wavelet constructions," in *Wavelet Applications in Signal and Image Processing III*, pp. 68–79, 1995.

25. W.Sweldens, "The lifting scheme: A construction of second generation wavelets," *SIAM Journal on Mathematical Analysis* **29**(2), pp. 511–546, 1998.

26. C. Roudet, F. Dupont, and A. Baskurt, "Multiresolution mesh segmentation based on surface roughness and wavelet analysis," *Visual Communications and Image Processing 2007* **6508**(1), p. 65082E, SPIE, 2007.

27. G. Lavou, F. Dupont, and A. Baskurt, "A new cad mesh segmentation method, based on curvature tensor analysis," *Computer-Aided Design* **37**(10), pp. 975–987, 2005.

28. D. Cohen-Steiner and J.-M. Morvan, "Restricted delaunay triangulations and normal cycle," in *SCG '03: Proceedings of the nineteenth annual symposium on Computational geometry*, pp. 312–321, ACM Press, (New York, NY, USA), 2003.

29. A. Said and W. A. Pearlman, "A new fast and efficient image codec based on set partitioning in hierarchical trees," *IEEE Transactions on Circuits and Systems for Video Technology* **6**, pp. 243–250, 1996.

30. C. Touma and C. Gotsman, "Triangle mesh compression.," in *Graphics Interface*, pp. 26–34, 1998.

31. http://www.cgal.org

32. N. Aspert, D. Santa-Cruz, and T. Ebrahimi, "Mesh: Measuring errors between surfaces using the hausdorff distance," in *Proceedings of the IEEE International Conference on Multimedia and Expo*, **I**, pp. 705 – 708, 2002. `http://mesh.epfl.ch`.

33. A. Golovinskiy, W. Matusik, H. Pfister, S. Rusinkiewicz, and T. Funkhouser, "A statistical model for synthesis of detailed facial geometry," *ACM Transactions on Graphics (Proc. SIGGRAPH)* **25**, July 2006.

34. M. X. Nguyen, X. Yuan, and B. Chen, "Geometry completion and detail generation by texture synthesis," *The Visual Computer (Special Issue for Pacific Graphics2005)* **21**(9–10), pp. 669–678, 2005.

35. Z.-Q. Cheng, H.-F. Liu, and S.-Y. Jin, "The progressive mesh compression based on meaningful segmentation," *Vis. Comput.* **23**(9), pp. 651–660, 2007.

36. S.-B. Park, C.-S. Kim, and S.-U. Lee, "Error resilient 3-d mesh compression," *IEEE Transactions on Multimedia* **8**, pp. 885–895, October 2006.

37. Z. Yan, S. Kumar, and C. C. J. Kuo, "Error-resilient coding of 3-d graphic models via adaptive mesh segmentation," *IEEE Trans. Circuits Syst. Video Techn.* **11**(7), pp. 860–873, 2001.

38. F. Payan and M. Antonini, "An efficient bit allocation for compressing normal meshes with an error-driven quantization," *Comput. Aided Geom. Des.* **22**(5), pp. 466–486, 2005.

39. C. Parisot, M. Antonini, and M. Barlaud, "High performance coding using a model-based bit allocation with EBCOT," in *EUSIPCO, XI European Signal Processing Conference*, (Toulouse, France), 3-6 septembre 2002.

40. D. C.-S. P. Alliez, O. Devillers, B. Levy, and M. Desbrun, "Anisotropic polygonal remeshing," *ACM Transactions on Graphics. Special issue for SIGGRAPH conference* , pp. 485–493, 2003.